Simultaneous Replacement of Asp-L210 and Asp-M17 with Asn Increases Proton Uptake by Glu-L212 upon First Electron Transfer to Q_B in Reaction Centers from *Rhodobacter sphaeroides*[†]

Eliane Nabedryk,*[,‡] Jacques Breton,[‡] Melvin Y. Okamura,[§] and Mark L. Paddock[§]

Section de Bioénergétique, CEA-Saclay, 91191 Gif-sur-Yvette, France, and Department of Physics, University of California at San Diego, La Jolla, California 92093

Received July 9, 2001; Revised Manuscript Received September 26, 2001

ABSTRACT: In the photosynthetic reaction center (RC) from *Rhodobacter sphaeroides*, the first electron transfer to the secondary quinone acceptor Q_B is coupled to the protonation of Glu-L212, located ∼5 Å from the center of Q_B. Upon the second electron transfer to Q_B, Glu-L212 is involved in fast proton delivery to the reduced Q_B. Since Asp-L210 and Asp-M17 play an important role in the proton transfer to the Q_B site [Paddock, M. L., Ädelroth, P., Chang, C., Abresch, E. C., Feher, G., and Okamura, M. Y. (2001) *Biochemistry 40*, 6893−6902], we investigated the effects of replacing one or both Asp residues with Asn on proton uptake by Glu-L212 using FTIR difference spectroscopy. Upon the first electron transfer to Q_B, the amplitude of the proton uptake by Glu-L212 at pH 8 is increased in the single and double mutant RCs, as is evident from the larger intensity (by 35−55%) of the carboxylic acid band at 1727 cm^{-1} in the Q_B^-/Q_B difference spectra of mutant RCs, compared to that at 1728 cm^{-1} in native RCs. This implies that the extent of ionization of Glu-L212 in the Q_B ground state is greater in the mutants than in native RCs and that Asp-M17 and Asp-L210 are at least partially ionized near neutral pH in native RCs. In addition, no changes in the protonation state or the environment of these two residues are detected upon Q_B reduction. The absence of the 1727 cm^{-1} signal in all of the RCs lacking Glu-L212, confirms that the positive band at 1728−1727 cm^{-1} probes the protonation of Glu-L212 in native and mutant RCs.

The reaction center (RC)[1] from the photosynthetic bacterium *Rhodobacter* (*Rb.*) *sphaeroides* uses light for the reduction and protonation of a bound quinone molecule Q_B (ubiquinone-10) to form quinol Q_BH_2 (*1*):

$$Q_B + 2e^- + 2H^+ \rightarrow Q_BH_2 \quad (1)$$

The double reduction of Q_B takes place in a two-step process, but only the second electron transfer leads to the direct protonation of the quinone. The details of the mechanism and energetics of proton-coupled electron transfer to the bound semiquinone Q_B^- and of the proton-transfer pathway(s) are still a matter of extensive studies (for a review, see *ref 2*). Effects of site-directed mutations in the RC from *Rb. sphaeroides* on the electron/proton-transfer rates showed that Asp-L213 (*3*−*5*), Ser-L223 (*6*), and Glu-L212 (*4*, *7*, *8*) are crucial for rapid electron/proton transfer to reduced Q_B, while mutations of acid residues located further from the Q_B site resulted in smaller effects on proton coupled electron transfer (*2*, *9*). In particular, Glu-L212 is important for the fast delivery of the second proton to the Q_B site (*7*, *8*, *10*). Although the first electron transfer to Q_B does not involve direct protonation of the quinone, it is accompanied by a fractional proton uptake by the RC protein (*11*−*13*). FTIR difference spectroscopy in combination with site-directed mutagenesis revealed that Glu-L212 participates directly to this partial proton uptake (*14*, *15*):

$$Q_A^-Q_B\text{—Glu-COO}^- + H^+ \rightarrow Q_AQ_B^-\text{—Glu-COOH} \quad (2)$$

In native RCs, proton uptake by Glu-L212 upon Q_B^- formation has been estimated to be 0.3−0.4 H^+/Q_B^- at pH 7 (*14*), indicating that there is a fraction [f(Glu-COO^-)] of RCs having Glu-L212 ionized in the Q_B ground state.

More generally, information about changes of the protonation states of internal carboxylic acid residues upon trigger-induced reactions can be directly obtained by using FTIR difference spectroscopy (*16*). Bands arising from the C═O stretching mode of protonated side chains of Asp and Glu appear in the region between 1770 and 1700 cm^{-1} and are sensitive to $^1H/^2H$ isotopic exchange (*17*). When the Q_B^- state is generated in native RCs from *Rb. sphaeroides* or *Rb. capsulatus*, the Q_B^- minus Q_B FTIR difference spectrum (Q_B^-/Q_B) displays a positive band at 1728 cm^{-1} that was attributed to substoichiometric proton uptake by Glu-L212 upon Q_B^- formation, based on its absence when Glu-L212

[†] This work was in part supported by the National Science Fundation (NSF MCB99-82186) and National Institutes of Health (NIH GM 41637 and NIH GM 13191).

* To whom correspondence should be addressed. Phone: 331 69 08 71 12. Fax: 331 69 08 87 17. E-mail: nabedryk@dsvidf.cea.fr.

[‡] Section de Bioénergétique.

[§] Department of Physics.

[1] Abbreviations: FTIR, Fourier transform infrared; RC, reaction center; Q_A, Q_B, primary, secondary quinone acceptor; H_A, bacteriopheophytin electron acceptor; H_B, bacteriopheophytin on the B-side; D, primary electron donor.

10.1021/bi011423w CCC: $20.00
Published on Web 10/26/2001

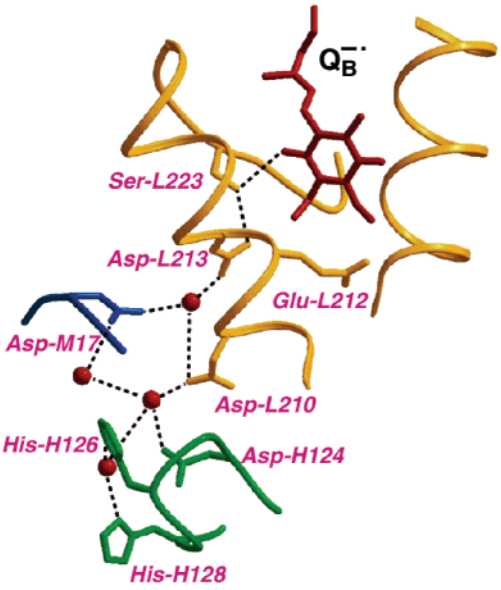

FIGURE 1: Part of the structure of the reaction center from *Rb. sphaeroides* showing the region between the proton entry point and Q_B^-. Located between the proton entry point and Glu-L212 are Asp-L210 and Asp-M17. In this study, we focus on mutations at these three sites (modified from ref *30* based on the structure reported in ref *25*).

was replaced with Gln (*14*, *15*, *18*, *19*). Previous steady-state FTIR studies of mutant RCs from *Rb. sphaeroides* led to the conclusion that neither Asp-L213, Asp-L210, nor Glu-H173 contribute significantly to the 1728 cm^{-1} peak (*14*, *20*, *21*).

The X-ray structures of the RC from *Rb. sphaeroides* show several putative proton pathways involving protonable residues and/or bound water molecules from the cytoplasm to Q_B (*22*−*26*). Recently, identification of a dominant proton pathway for the transfer of both the first and the second proton to reduced Q_B has been achieved (*10*, *27*, *28*). The entry point for the protons is located at the surface of the RC H-subunit, near His-H126, His-H128, and Asp-H124 that bind metal ions such as Cd^{2+} and Zn^{2+} (*29*). Located in the region between the proton entry point and Q_B (Figure 1) are Asp-M17 and Asp-L210, and it has been proposed that they act in parallel for efficient proton transfer to Q_B^-. Simultaneous replacement of these two residues by Asn drastically slowed the rate of proton transfer (*30*) while the effect of the single mutation of Asp-L210 or Asp-M17 to Asn was small (*28*). However, in the presence of Cd^{2+} bound to RCs, the single mutation of Asp-L210 or Asp-M17 to Asn significantly decreases the rate of proton transfer, which shows the important role that Asp-L210 and Asp-M17 play in the proton-transfer chain (*28*).

In the present work, using steady-state light-induced FTIR difference spectroscopy, we compare at pH 8 the effects of the double DN(L210)/DN(M17) and single DN(L210) and DN(M17) mutations in RCs from *Rb. sphaeroides* on proton uptake by Glu-L212 upon Q_B^- formation. We also investigate the introduction of the additional mutation Glu L212 → Gln leading to the triple EQ(L212)/DN(L210)/DN(M17) and double EQ(L212)/DN(L210) mutant RCs. Information about the ionization state of Asp-M17 and Asp-L210 in the ground state of native RCs is provided by examining the effect of mutations on the amplitude of the 1728 cm^{-1} band which is used as a probe of the local electrostatic environment. A preliminary account of this work has been presented (*31*).

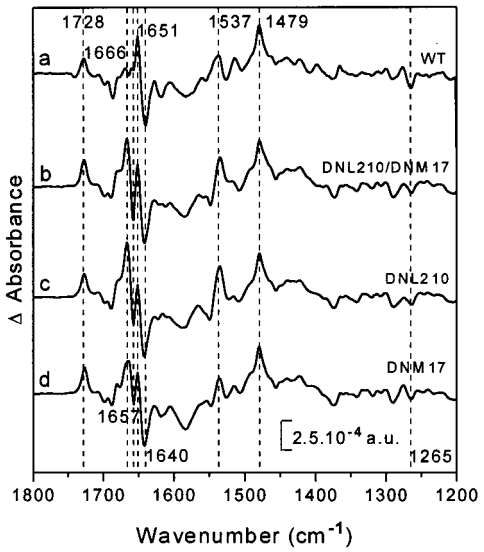

FIGURE 2: Light-induced Q_B^-/Q_B FTIR difference spectra of wild-type (a) and mutant (b−d) RCs from *Rb. sphaeroides* in ^1H_2O at pH 8, 15 °C. (b) The double mutant DN(L210)/DN(M17); (c) the single mutant DN(L210); (d) the single mutant DN(M17). Note the increase of the 1728 cm^{-1} peak in the mutant RCs compared to native RCs. About 60 000 scans were averaged. Spectral resolution was 4 cm^{-1}. a.u., absorbance units. The frequencies indicated at the top (bottom) of the figure correspond to positive (negative) IR peaks.

EXPERIMENTAL PROCEDURES

The construction of the site-directed mutants is described in refs *28* and *30*. RC isolation was performed as reported in ref *5*. A detailed description of the preparation of RC samples for FTIR experiments is given in refs *14* and *21*: 10 μL of an RC sample (~0.2 mM) containing an excess of ubiquinone was deposited on a CaF_2 disk; then, 10 μL of ascorbate (10 mM) and diaminodurene (2,3,5,6-tetramethyl-*p*-phenylenediamine), 20 mM in Tris-HCl, pH 8, 90 mM, was added. The RC sample was dried to a thin paste then covered with 2 μL of ^1H_2O and sealed with another CaF_2 disk. The preparation of RC samples in ^2H_2O was carried out as reported in ref *21*.

Steady-state light-induced FTIR difference spectra of the Q_B to Q_B^- transition in native and mutant RCs were recorded at 15 °C in ^1H_2O or ^2H_2O, with a Nicolet 60SX spectrometer, as described in refs *14* and *21*. The Q_B^- state was generated by excitation with a single saturating flash (Nd:YAG laser, 7 ns, 530 nm). Difference spectra were calculated from each of 128 scans (acquisition time: 23 s) recorded before and after laser flash excitation. For a given sample, these measurements were repeated over 15−20 h. Spectra are an average of two to three samples.

RESULTS

The data are broken into two groups for presentation. The first group, consisting of native RCs, the double DN(L210)/DN(M17) mutant and the corresponding single mutants, retains Glu-L212. The second group, consisting of EQ(L212), EQ(L212)/DN(L210), and EQ(L212)/DN(L210)/DN(M17) RCs, has Glu replaced with Gln at L212. Figures 2 and 3

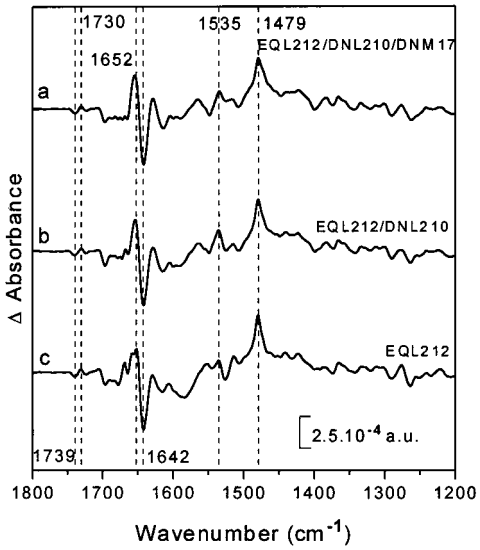

FIGURE 3: Light-induced Q_B^-/Q_B FTIR difference spectra of mutant RCs from *Rb. sphaeroides* in ^1H_2O at pH 8, 15 °C. (a) The triple mutant EQ(L212)/DN(L210)/DN(M17); (b) the double mutant EQ(L212)/DN(L210); (c) the single mutant EQ(L212). Note the absence of the 1728 cm^{-1} peak in the mutant RCs lacking Glu-L212. Same conditions as in Figure 2.

Table 1: Main Vibrational IR Frequencies (cm^{-1}) in Native RCs

positive peaks		negative peaks	
1728	Glu-L212 COOH (νC═O)	1740	H_B, 10a ester C═O[a]
		1685	Glu L212 amide I[a]
1651	amide I/side chain	1640	amide I/side chain, Q_B (νC═O)
1479	semiquinone Q_B^- (νC···O)	1617	Q_B (νC═C), side chain
		1290, 1265	Q_B (C−O−CH_3)
1537	amide II (δNH)	1527	amide II

[a] Tentative assignment.

show the Q_B^-/Q_B light-induced FTIR difference spectra corresponding to the first and second groups of RCs, respectively. In native RCs (Figure 2a, Table 1), most of the main negative and positive bands have been previously attributed to modes of chemical groups belonging to the quinone, the semiquinone, and the protein (*14*, *32*, *33*). The Q_B^-/Q_B spectra of all the mutant RCs display typical absorption changes associated with first electron transfer to Q_B, notably the major peaks at ∼1651 cm^{-1} (+), ∼1641 cm^{-1} (−), and 1479 cm^{-1} (+), as well as several other common features, e.g., at ∼1290 cm^{-1} (−), 1265 cm^{-1} (−), and 1535−1537 cm^{-1} (+). Thus, as observed in native RCs, the main absorption band of the semiquinone Q_B^- peaks at 1479 cm^{-1} (νC···O) in ^1H_2O and at 1481 cm^{-1} in ^2H_2O (data not shown) in all the mutant spectra. This indicates that the interactions between Q_B^- and the surrounding amino acid residues are comparable in native and mutant RCs. The ∼1651/1641 cm^{-1} differential signal, which is comparable in all RCs, lies in the amide I (νC═O), side chains, and νC═O Q_B (at 1641 cm^{-1}, see refs *33* and *34*) range. The amide II mode (δN−H and νC−N) of the mutant spectra contributes at 1548−1549/1535−1537 cm^{-1} with, however, a variable amplitude in each mutant: the largest one is observed in the DN(L210)/DN(M17) and DN(L210) mutants RCs and the smallest one in the EQ(L212) mutant RCs. As previously described in refs *14* and *21*, all the spectra (Figures 2−5) were normalized with respect to the semi-

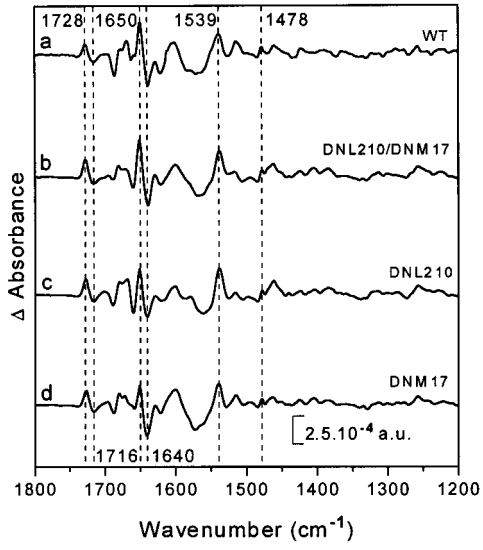

FIGURE 4: Calculated double difference spectra between Q_B^-/Q_B difference spectra of *Rb. sphaeroides* RCs obtained in ^1H_2O and ^2H_2O (^1H_2O minus ^2H_2O). (a) Wild-type; (b) DN(L210)/DN(M17); (c) DN(L210); (d) DN(M17). Note the shift of the 1728 cm^{-1} peak in ^1H_2O to 1716 cm^{-1} in ^2H_2O.

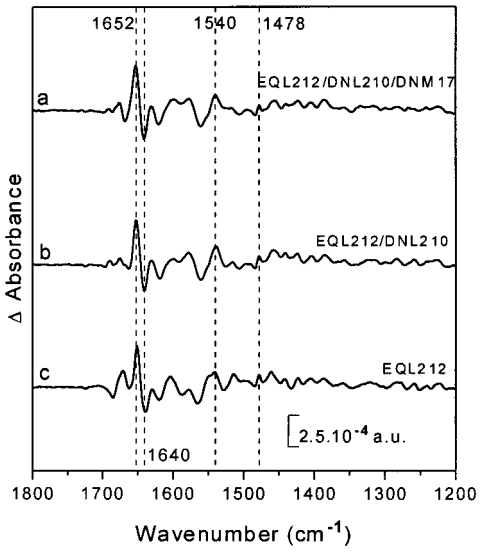

FIGURE 5: Calculated double difference spectra between Q_B^-/Q_B difference spectra of *Rb. sphaeroides* RCs obtained in ^1H_2O and ^2H_2O (^1H_2O minus ^2H_2O). (a) EQ(L212)/DN(L210) /DN(M17); (b) EQ(L212)/DN(L210); (c) EQ(L212). Note the absence of significant features above 1700 cm^{-1}.

quinone band at 1479 cm^{-1} and the bands at 1290 and 1265 cm^{-1} arising in part from C−O−C modes of the quinone methoxy groups (*32*).

With respect to native RCs, the Q_B^-/Q_B spectra of the mutant RCs display several changes. In the first set of spectra (Figure 2) which includes the double mutant DN(L210)/DN(M17) and the two corresponding single mutants, a new intense differential feature is observed at 1666−1665/1657 cm^{-1} together with a common differential signal at 1548/1537 cm^{-1}. In addition, the amplitude of the positive peak at 1727 cm^{-1} in these mutants is larger than that at 1728 cm^{-1} in native RCs, while the small negative signal seen at 1740 cm^{-1} in native RCs is lacking. It is worth noting that the spectra of the three mutants are closely comparable in the whole 1800−1200 cm^{-1} range, with the largest resem-

blance between the DN(L210)/DN(M17) and DN(L210) spectra.

The second set of spectra (Figure 3) includes the three mutants that have Glu replaced with Gln at L212. The overall shape of these spectra is also closely comparable to each other, with the largest resemblance occurring between the double EQ(L212)/DN(L210) and triple EQ(L212)/DN(L210)/DN(M17) RCs spectra. The carboxylic acid signal peaking at 1728 cm^{-1} in native RCs (Figure 2a) is lacking in all the mutants that contain Gln at the L212 site (Figure 3), in agreement with previous data obtained with the single EQ(L212) and the double EQ(L212)/DN(L213) mutant RCs (*14*). Instead, a small differential signal is observed at 1739 (−)/1730 (+) cm^{-1}. Furthermore, the introduction of the EQ(L212) mutation prevents the appearance of the large differential signal observed at 1666/1657 cm^{-1} in the DN(L210)/DN(M17) and DN(L210) mutants.

The Q_B^-/Q_B difference spectra were also obtained in ^2H_2O to identify bands that are sensitive to $^1H/^2H$ exchange. Figures 4 and 5 show the Q_B^-/Q_B double difference spectra (Q_B^-/Q_B difference spectra obtained in ^1H_2O minus Q_B^-/Q_B difference spectra obtained in ^2H_2O) corresponding to the first and the second groups of mutant RCs, respectively. For each group of mutants, the overall shape of the double difference spectra is comparable, indicating that most of the absorption changes arise from the same chemical bonds. Moreover, the double difference spectra of DN(L210)/DN(M17), DN(L210), and DN(M17) mutant RCs are comparable to those of native RCs, with a differential signal at ∼1650/1640 cm^{-1} and a positive signal at 1539 cm^{-1}, most probably due to protein modes (amide I and amide II, respectively). The 1666−1665/1657 cm^{-1} differential signal which is unique to the spectra of DN(L210) and/or DN(M17) mutants (Figure 2) is not significantly shifted (at most by 1 cm^{-1}) in ^2H_2O (Figure 4). Importantly, a similar frequency downshift of the band at 1728−1727 cm^{-1} in ^1H_2O to ∼1716 cm^{-1} in ^2H_2O is observed for the first series of mutants and native RCs (Figure 4). In native RCs, the differential signal at 1728/1717 cm^{-1} in the double difference spectra has been previously attributed to the $^1H/^2H$ effect on the C═O stretching mode of the protonated side chain of Glu-L212 (*14*).

The overall shape of the double difference spectra (^1H_2O minus ^2H_2O) corresponding to the second group of mutants containing the EQ(L212) mutation (Figure 5) is also comparable with a main differential signal at ∼1652/1640 cm^{-1} (amide I) and a positive band at 1540 cm^{-1} (amide II). It has to be noticed that the region above 1700 cm^{-1} is essentially flat, which indicates that the small differential signal observed at 1739/1730 cm^{-1} in ^1H_2O in these mutants (Figure 3) is not sensitive to $^1H/^2H$ exchange, as previously reported for the single EQ(L212) and the double EQ(L212)/DN(L213) mutant RCs (*14*).

DISCUSSION

In the present work, we investigate the importance of Asp-L210 and Asp-M17 for the proton uptake process by the RC protein on Q_B^- formation. We report the Q_B^-/Q_B FTIR difference spectra at pH 8 from the single, double, and triple mutant RCs in which Asp-L210 and/or Asp-M17 was replaced with Asn and Glu-L212 with Gln. Information about the ionization state of these carboxylic acids in the Q_B and Q_B^- states in native RCs and their involvement in proton uptake in response to the formation of Q_B^- is obtained. The effect of the single and double mutations on proton uptake by Glu-L212 is determined.

Protein Rearrangement: Contribution of Asn-L210 and Asn-M17. Any contributions of the Asn side chains to the FTIR difference spectrum are expected in the 1670−1680 cm^{-1} (νC═O) and 1612−1622 cm^{-1} (δNH_2) ranges (*35*, *36*). In the νC═O range, the Q_B^-/Q_B difference spectra of DN(L210) and DN(L210)/DN(M17) RCs show a new intense differential signal at 1666/1657 cm^{-1} (Figure 2) with a comparable amplitude for both mutants. This signal is downshifted by ∼ 1 cm^{-1} in ^2H_2O. The Q_B^-/Q_B spectrum of DN(M17) RCs (Figure 2) exhibits a smaller (∼2-fold) signal at 1665/1657 cm^{-1}. Although this new 1666−1665/1657 cm^{-1} signal could also arise from a conformational change of the side chain of Asn-L210 and/or Asn-M17, its frequency would be ∼10 cm^{-1} downshifted with respect to the side-chain absorption band of model compounds of Asn in ^1H_2O (*35*, *36*) and the ∼1 cm^{-1} frequency downshift of this signal upon $^1H/^2H$ exchange disfavors such an assignment.[2] The band is more compatible with an assignment to a change in the νC═O peptide (*38*) upon Q_B^- formation suggesting that the backbone is more flexible in the first group of mutants than in native RCs. This amide I signal could result from either a localized perturbation of the backbone at Asn-L210 and/or Asn-M17 or from a delocalized perturbation over several peptide groups. In support of such an assignment, a differential signal at 1548/1535 cm^{-1} lying in the amide II range is unique to the mutants with Asn-L210 and/or Asn-M17. It is worth noting that such a conformational change at 1666−1665/1657 cm^{-1} does not occur upon Q_B reduction in the triple EQ(L212)/DN(L210)/DN(M17) and double EQ(L212)/DN(L210) mutant RCs (Figure 3).

In addition to the peptide C═O groups and the Asn side chains, several other non-carboxylic amino acid residues (Gln, Arg, Lys) can contribute to the spectral region 1700−1600 cm^{-1} (*35*, *36*) in which other small differences are observed in the mutant RCs. The 1622−1612 cm^{-1} spectral range of the DN(L210)/DN(M17) and DN(L210) mutants shows two very small negative peaks at 1621 and 1612 cm^{-1} and 1622 and 1610 cm^{-1}, respectively, instead of the unique negative band seen at 1617 cm^{-1} in native RCs which in part arises from the νC═C of Q_B (Table 1, ref *33*). One of the small features seen in the 1622−1612 cm^{-1} range of the spectra displayed in Figure 2, panels b and c, could arise from the δNH_2 mode of Asn-L210 side chain (*35*, *36*).

While the single DN(M17) mutation gives rise to new features in the Q_B^-/Q_B spectrum compared to that of native RCs, combining it with changes at L210 [DN(L210)/DN(M17) and EQ(L212)/DN(L210)/DN(M17)] does not result in the same additional IR absorption changes. The Q_B^-/Q_B spectra of DN(L210)/DN(M17) and EQ(L212)/DN(L210)/DN(M17) RCs are comparable to those of DN(L210) and

[2] The only study of model compounds in ^2H_2O performed so far reported that Asn gives rise to a band at 1648 cm^{-1} referred to the νC═O of the side chain (*37*), thus suggesting a frequency downshift by 30 cm^{-1} upon $^1H/^2H$ exchange, which appears very large for a νC═O mode.

EQ(L212)/DN(L210) RCs, respectively. In contrast to the DN(M17) single mutant, the replacement of Asp-M17 with Asn in the double and triple mutants is quite silent and does not add to further structural rearrangements.

In common, the Q_B^-/Q_B spectra of native and mutant RCs all exhibit a characteristic differential signal in the amide I range at ~1651/1640 cm^{-1} (Figures 2 and 3). Such a peptide C═O signature, the 1651 cm^{-1} frequency of which is typical of α-helical structure, most probably reflects a small protein structural change common to all native and mutant RCs that could be involved in the stabilization of the charge on Q_B.

Proton Uptake by Glu-L212 in Asn-L210 and Asn-M17 Mutants RCs. The FTIR spectra displayed in Figure 2 show a prominent positive band at 1727−1728 cm^{-1} in the expected region for a protonating carboxylate. In native RCs, this band has been previously assigned to the νC═O side-chain mode of protonated Glu-L212 (*14*), which is further supported by results from this paper (see above). The band probes the protonation of Glu-L212 upon Q_B reduction resulting from the electrostatic interaction between Q_B^- and the partly ionized form of Glu-L212.

This FTIR band is observed in all mutant RCs which have Glu at L212 (Figure 2). The band is shifted to 1716 cm^{-1} in ^2H_2O (Figure 4). The similarity of the 1727 cm^{-1} (^1H_2O) and 1716 cm^{-1} (^2H_2O) bands in the first group of mutant spectra to those in the native RCs indicates that (1) the carboxylic acid band at 1727 cm^{-1} in these mutants can be attributed to protonation of Glu-L212 since it is present in all mutant (and native) RCs that retain Glu-L212 and is absent in all mutant RCs lacking Glu at L212 (reported above and in ref *14*); (2) the 1 cm^{-1} frequency downshift with respect to native RCs is attributed to a little difference in the environment of the protonated side chain of Glu-L212 in the mutant RCs; (3) Asp-L210 and Asp-M17 do not contribute to the 1728 cm^{-1} band observed in native RCs. Furthermore, the amplitude of the proton uptake by Glu-L212 is increased in the L210/M17 mutant RCs, as seen by the larger intensity of the band at 1727 cm^{-1} in DN(L210)/DN(M17) (~55%), DN(M17) (~45%), and DN(L210) (~35%) RCs than that at 1728 cm^{-1} in native RCs. In these mutant RCs, the equilibrium fraction of RCs having Glu-L212 ionized in the Q_B ground state is therefore increased. A larger protonation of Glu-L212 has been previously observed for several other mutant RCs from *Rb. sphaeroides*, e.g., in the Asp-L213 → Asn and Glu-H173 → Gln mutant RCs (*14*, *21*).

In all the mutants containing the EQ(L212) mutation (Figures 3 and 5), the small differential signal at 1739/1730 cm^{-1} in ^1H_2O, which is not significantly sensitive to $^1H/^2H$ exchange, is not assigned to a perturbation of carboxylic acid group(s). FTIR studies of the photoreduction of Q_A (primary quinone electron acceptor) and H_A (bacteriopheophytin electron acceptor) in mutant RCs from *Rb. sphaeroides* (*39*) *and Rhodopseudomonas* (*Rp.*) *viridis* (*40*) bearing mutations near H_A have shown that the reduction of Q_A induced a pronounced electrostatic effect on the molecular vibration(s) of the 10a-ester C═O of H_A above 1700 cm^{-1}. In *Rp. viridis* RCs, an electrochromic shift of the 10a-ester C═O of H_A has been also detected upon Q_B reduction, although with a smaller amplitude than upon Q_A reduction (*41*). As previously suggested in ref *14* for the single EQ(L212) and the double EQ(L212)/DN(L213) mutant RCs (as well as for the small negative signal at 1740 cm^{-1} in native RCs, Figure 2a, Table 1), the differential signal observed at 1739/1730 cm^{-1} in the second group of spectra (Figure 3) could similarly account for the electrostatic influence of the presence of an electron on Q_B on the IR mode of the 10a-ester C═O of H_B. Such a carbonyl perturbation (electric field and/or orientation change) does not occur in the first group of mutants retaining Glu-L212 (Figure 2). Moreover, the absence of the differential signal at 1739/1730 cm^{-1} in the double DN(L210)/DN(M17) and single DN(L210) and DN(M17) mutant RCs appears correlated with the presence of the conformational change occurring in these mutants at 1666−1665/1657 cm^{-1}. Reciprocally, no backbone change takes place at 1666−1665/1657 cm^{-1} in the triple EQ(L212)/DN(L210)/DN(M17) and double EQ(L212)/DN(L210) mutant RCs while the differential signal that could reflect an electrochromic shift of the 10a-ester C═O of H_B is indeed observed when Q_B is reduced.

Protonation State of Asp-M17 and Asp-L210 in Native RCs. In the Q_B^-/Q_B spectra of native RCs at pH 7−8, no band above 1700 cm^{-1} can be assigned to a signature of protonated Asp-L210 and Asp-M17. Consequently, the FTIR data suggest no significant change near neutral pH in the ionization state or the environment of these two Asp residues upon Q_B reduction. This result is somewhat surprising since Asp-L210 and Asp-M17 belong to a cluster of protonable residues located near Q_B and that the electrostatic interactions between the components of the cluster (six carboxylic acids, three basic residues, and three water molecules) are expected to be important (*24*). It has been proposed that one or more protons would likely be bound and shared among the different components (*24*). As discussed in ref *42*, it cannot be excluded that some carboxylic acid residues involved in proton uptake/release by the RC when Q_B is reduced give rise to broad bands difficult to detect or absorb outside their normal IR frequency range and are shifted to a lower frequency and hence hidden by other FTIR signals. Another possibility would be that the proton(s) shared by the coupled carboxylic acids of the cluster in the Q_B ground state rearrange over the different acids in the Q_B^- state without changing the final net charge in the cluster. In this case, if the delocalized proton gives rise to a single IR band, only a small (if any) IR change would be expected due to internal proton rearrangement. Finally, it might be also possible that the proton resides at least in part at bound water molecule(s). IR signature for a highly polarizable hydrogen-bonding network involving protonated water molecules ($H_5O_2^+$) possibly bonded to carboxyl groups has been previously detected in native RCs from *Rb. sphaeroides* as an increase of absorption at ~2600 cm^{-1} upon Q_B reduction (*42*).

Information about the protonation state of Asp-L210 and Asp-M17 in the ground state of native RCs can be further provided by examining the effect of mutations on the amplitude of the 1727 cm^{-1} band which should respond to changes in the local electrostatic environment. The larger amplitude of the 1727 cm^{-1} band in DN(L210)/DN(M17), DN(L210), and DN(M17) mutant RCs, compared to that at 1728 cm^{-1} in native RCs, is attributed to the replacement of a negatively charged Asp at L210 and/or at M17 with a neutral side chain, leading to a greater protonation of Glu-L212. This implies that, in native RCs, Asp-M17 and Asp-L210 are at least partially ionized near neutral pH, in

agreement with kinetic electron-transfer results (*28*, *30*). FTIR data also suggest that the pK_a of Asp-L210 and Asp-M17 should be different in native RCs (pK_a Asp-M17 < pK_a Asp-L210) since the intensity of the 1727 cm^{-1} band is significantly larger in DN(M17) than in DN(L210). In addition, the replacement of both Asp with Asn leads to a further increase in the 1727 cm^{-1} band, although not in an additive manner.

Comparison with Other Studies. In transient optical studies, the charge recombination rate, k_{BD}, for the reaction $D^+Q_AQ_B^- \rightarrow DQ_AQ_B$, which is correlated to the stability of the Q_B^- state, is expected to change as a function of the effect of the mutations on the electrostatic environment near Q_B, i.e., the more positive the electrostatic potential near Q_B, the slower the observed k_{BD} rate (*43*). In agreement with the replacement of one or two (partly) negatively charged residues with neutral side chains in the mutants at L210/M17 site(s), the k_{BD} values are decreased up to 2-fold in the mutant RCs (*30*). As a consequence of the more positive electrostatic potential near Glu-L212 (and Q_B^-) in the L210/M17 mutants, Glu-L212 is expected to be more ionized prior to Q_B^- formation in the mutant RCs than in native RCs. Indeed, the increased amplitude of the proton uptake by Glu-L212 upon Q_B reduction in the single and double mutants, as is evident from the present data, is attributed to a greater fraction of ionized Glu-L212 in the ground state. Thus, there is a qualitative agreement between the decrease of the charge recombination rate previously reported from optical kinetic measurements (*30*) and the increase of the protonation of Glu-L212 reported above from FTIR measurements. Also, the slower measured rate constant $k_{AB}^{(1)}$ at pH 8 for the first electron transfer to Q_B (eq 2) in the single and double mutant RCs (*28*, *30*) is consistent with a change in the ionization state of Glu-L212 in the ground state in these mutants. Furthermore, time-resolved FTIR study of the electron-transfer reaction $Q_A^-Q_B \rightarrow Q_AQ_B^-$ in the double mutant shows that protonation of Glu-L212 upon Q_B^- formation is also slow and proceeds at the same kinetics as reduction of Q_B (ref *44*, and manuscript in preparation).

Recent electrostatic calculations in RCs from *Rb. sphaeroides* (*45*, *46*) show that a cluster of acids, formed by Asp-L210, Asp-L213, and Glu-L212, shares one proton in the Q_B state and two protons in the Q_B^- state. Upon Q_B^- formation, the protonation changes occur either at Asp-L210 and Asp-L213 according to Alexov and Gunner (*45*) or at Glu-L212 and Asp-L213 according to Rabenstein et al. (*46*). Molecular dynamics simulations of the binding of Q_B and Q_B^- also imply changes of protonation state of Glu-L212/Asp-L213 with the uptake of one proton on reduction of Q_B (*47*). The present FTIR data agree well with the results reported in (*46*), since it was calculated that in native RCs the protonation changes occur mainly at Glu-L212 while the change is very small at Asp-L213.

In conclusion, the present work shows no evidence for a significant contribution of Asp-L210 and/or Asp-M17 near neutral pH to proton uptake/release on Q_B^- formation in RCs from *Rb. sphaeroides*. However, replacement of either one or both of these two Asp residues with Asn changes the ionization state of Glu-L212 in the ground state and increases the extent of proton uptake by Glu-L212 upon first electron transfer to Q_B. Proton transfer/rearrangement within the acid cluster near Q_B (which includes Asp-L210 and Asp-M17, ref *24*), upon Q_B reduction could possibly contribute to the positive IR continuum seen at ~2600 cm^{-1} in native RCs (*42*), but it is not visible in the normal IR frequency range of protonated carboxylic groups (1770−1700 cm^{-1}). Taking into account our previous FTIR data obtained on the mutants at Asp-L213, Glu-L212, and Glu-H173 (*14*, *20*, *21*) and the present FTIR work on the mutants at Asp-L210, Asp-M17, and Glu-L212, we conclude that proton binding by Glu-L212 is the only contributor to the classic carboxylic acid IR band, thus emphasizing the unique behavior of Glu-L212 in the first electron-transfer reaction in native RCs. The fraction of RCs having Glu-L212 ionized in the Q_B ground state would be modulated by neighboring acid residues, such as Asp-L210 and Asp-M17.

ACKNOWLEDGMENT

We thank Winfried Leibl for helpful discussions and critical comments on the manuscript, Sébastien Quesson for help in preparing Figures 2−5, and Ed Abresch and Charlene Change for technical assistance.

REFERENCES

1. Feher, G., Allen, J. P., Okamura, M. Y., and Rees, D. C. (1989) *Nature 339*, 111−116.
2. Okamura, M. Y., Paddock, M. L., Graige, M. S., and Feher, G. (2000) *Biochim. Biophys. Acta 1458*, 148−163.
3. Takahashi, E., and Wraight, C. A. (1990) *Biochim. Biophys. Acta 1020*, 107−111.
4. Takahashi, E., and Wraight, C. A. (1992) *Biochemistry 31*, 855−866.
5. Paddock, M. L., Rongey, S. H., McPherson, P. H., Juth, A., Feher, G., and Okamura, M. Y. (1994) *Biochemistry 33*, 734−745.
6. Paddock, M. L., McPherson, P. H., Feher, G., and Okamura, M. Y. (1990) *Proc. Natl. Acad. Sci. U.S.A. 87*, 6803−6807.
7. Paddock, M. L., Rongey, S. H., Feher, G., and Okamura, M. Y. (1989) *Proc. Natl. Acad. Sci. U.S.A. 86*, 6602−6606.
8. McPherson, P., H., Schönfeld, M., Paddock, M. L., Okamura, M. Y., and Feher, G. (1994) *Biochemistry 33*, 1181−1193.
9. Takahashi, E., and Wraight, C. A. (1996) *Proc. Natl. Acad. Sci. U.S.A. 93*, 2640−2645.
10. Ädelroth, P., Paddock, M. L., Sagle, L. B., Feher, G., and Okamura, M. Y. (2000) *Proc. Natl. Acad. Sci. U.S.A. 97*, 13086−13091.
11. Maróti, P., and Wraight, C. A. (1988) *Biochim. Biophys. Acta 934*, 329−347.
12. McPherson, P. H., Okamura, M. Y., Feher, G. (1988) *Biochim. Biophys. Acta 934*, 348−368.
13. Miksovska, J., Schiffer, M., Hanson, D. K., and Sebban, P. (1999) *Proc. Natl. Acad. Sci. U.S.A. 96*, 14348−14353.
14. Nabedryk, E., Breton, J., Hienerwadel, R., Fogel, C., Mäntele, W., Paddock, M. L., and Okamura, M. Y. (1995) *Biochemistry 34*, 14722−14732.
15. Hienerwadel, R., Grzybek, S., Fogel, C., Kreutz, W., Okamura, M., Y., Paddock, M. L., Breton, J., Nabedryk, E., and Mäntele, W. (1995) *Biochemistry 34*, 2832−2843.
16. Mäntele, W. (1993) *Trends Biochem. Sci. 18*, 197−202.
17. Siebert, F. (1993) in *Biomolecular Spectroscopy* (Clark, R. J. H., and Hester, R. E., Eds.) Part A, pp 1−54, John Wiley & Sons, New York.
18. Nabedryk, E. (1999) *Biochim. Biophys. Acta 1411*, 206−213.
19. Nabedryk, E., Breton, J., Joshi, H. M., and Hanson, D. K. (2000) *Biochemistry 39*, 14654−14663.
20. Nabedryk, E., Breton, J., Hienerwadel, R., Fogel, C., Mäntele, W., Paddock, M. L., and Okamura, M. Y. (1995) in *Photosynthesis: from Light to Biosphere* (Mathis, P., Ed.) Vol. I, pp 875−878, Kluwer Academic Publishers, Dordrecht.
21. Nabedryk, E., Breton, J., Okamura, M. Y., and Paddock, M. L. (1998) *Biochemistry 37*, 14457−14462.

22. Ermler, U., Fritzsch, G., Buchanan, S. K., and Michel, H. (1994) *Structure 2*, 925−936.
23. Lancaster, C. R. D., Ermler, U., and Michel, H. (1995) in *Anoxygenic Photosynthetic Bacteria* (Blankenship, R. E., Madigan, M. T., and Bauer, C. E., Eds.) pp 503−525, Kluwer Academic Publishers, Dordrecht.
24. Abresch, E. C., Paddock, M. L., Stowell, M. H. B., McPhillips, T. M., Axelrod, H. L., Soltis, S. M., Rees, D. C., Okamura, M. Y., and Feher, G. (1998) *Photosynth. Res. 55*, 119−125.
25. Stowell, M. H. B., McPhillips, T. M., Rees, D. C., Soltis, S. M., Abresch, E., and Feher, G. (1997) *Science 276*, 812−816.
26. Fritzsch, G., Kampmann, L., Kapaun, G., and Michel, H. (1998) *Photosynth. Res. 55*, 1−6.
27. Paddock, M. L., Graige, M. S., Feher, G., and Okamura, M. Y. (1999) *Proc. Natl. Acad. Sci. U.S.A. 96*, 6183−6188.
28. Paddock, M. L., Feher, G., and Okamura, M. Y. (2000) *Proc. Natl. Acad. Sci. U.S.A. 97*, 1548−1553.
29. Axelrod, H. L., Abresch, E. C., Paddock, M. L., Okamura, M. Y., and Feher, G. (2000) *Proc. Natl. Acad. Sci. U.S.A. 97*, 1542−1547.
30. Paddock, M. L., Ädelroth, P., Chang, C., Abresch, E. C., Feher, G., and Okamura, M. Y. (2001) *Biochemistry 40*, 6893−6902.
31. Nabedryk, E., Breton, J., Okamura, M., Y., and Paddock, M., L. (2001) *Biophys. J. 80*, 427a.
32. Breton, J., Berthomieu, C., Thibodeau, D. L., and Nabedryk, E. (1991) *FEBS Lett. 288*, 109−113.
33. Breton, J., Boullais, C., Berger, G., Mioskowski, C., and Nabedryk, E. (1995) *Biochemistry 34*, 11606−11616.
34. Brudler, R., de Groot, H. J. M., van Liemt, W. B. S., Gast, P., Hoff, A. J., Lugtenburg, J., and Gerwert, K. (1995) *FEBS Lett. 370*, 88−92.
35. Venyaminov, S. Yu., and Kalnin, N. N. (1990) *Biopolymers 30*, 1243−1257.
36. Rahmelow, K., Hübner, W., and Ackermann, Th. (1998) *Anal. Biochem. 257*, 1−11.
37. Chirgadze, Yu. N., Fedorov, O. V., and Trushina, N. P. (1975) *Biopolymers 14*, 679−694.
38. Goormaghtigh, E., Cabiaux, V., and Ruysschaert, J.-M. (1994) in *Subcellular Biochemistry: Physicochemical Methods in the Study of Biomembranes* (Hilderson, H. J., and Ralston, G. B., Eds.) Vol. 23, pp 329−362. Plenum Press, New York.
39. Breton, J., Nabedryk, E., Allen, J. P., and Williams, J. C. (1997) *Biochemistry 36*, 4515−4525.
40. Breton, J., Bibikova, M., Oesterhelt, D., and Nabedryk, E. (1999) *Biochemistry 38*, 11541−11552.
41. Breton, J., Bibikova, M., Oesterhelt, D., and Nabedryk, E. (1998) in *Photosynthesis: Mechanisms and Effects* (Garab, G., Ed.) Vol. II, pp 687−692, Kluwer Academic Publishers, Dordrecht.
42. Breton, J., and Nabedryk, E. (1998) *Photosynth. Res. 55*, 301−307.
43. Paddock, M. L., Feher, G., and Okamura, M. Y. (1997) *Biochemistry 36*, 14238−14249.
44. Mezzetti, A., Nabedryk, E., Breton, J., Okamura, M. Y., Paddock, M., L., and Leibl, W. (2001) *Biophys. J. 80*, 428a.
45. Alexov, E. G., and Gunner, M. R. (1999) *Biochemistry 38*, 8253−8270.
46. Rabenstein, B., Ullmann, G. M., and Knapp E.-W. (2000) *Biochemistry 39*, 10487−10496.
47. Grafton, A. K., and Wheeler, R. A. (1999) *J. Phys. Chem. B 103*, 5380−5387.

BI011423W